Far-field breakup of spiral waves in the plankton ecological systems

Quan-Xing Liu,[1] Bai-Lian Li,[2] and Zhen Jin[1, *]

[1]*Department of Mathematics, North University of China,*
Taiyuan, Shan'xi 030051, People's Republic of China
[2]*Ecological Complexity and Modeling Laboratory,*
University of California, Riverside, CA 92521-0124, USA
(Dated: August 10, 2013)

Alexander B. Medvinsky *et al* [A. B. Medvinsky, I. A. Tikhonova, R. R. Aliev, B.-L. Li, Z.-S. Lin, and H. Malchow, Phys. Rev. E **64**, 021915 (2001)] show that the minimal reaction-diffusion model of phytoplankton-zooplankton can exhibit both regular and chaotic behavior, and spatiotemporal patterns in a patchy environment. Basing on that, the spatial plankton model is further investigated numerically in this paper when system within the mixed Turing-Hopf bifurcation region. We find that the spiral waves exist in that region, exhibit far-field breakup of the spiral waves over large ranges of diffusion coefficients of phytoplankton and zooplankton. Our results show that far-field breakup of spiral waves also exists in the oceanic ecological systems. Moreover, the far-field breakup of spiral waves also lead to the spatial chaos patterns, but it does not gradually involve the whole space within the large ranges of diffusion coefficients of phytoplankton and zooplankton. The far-field breakup spiral waves leading to spatial chaos patterns may be useful to understand the population dynamics of oceanic ecological systems.

I. INTRODUCTION

There is a growing interest in the spatial pattern dynamics of ecological systems [1, 2, 3, 4, 5, 6, 7, 8, 9, 10, 11, 12, 13]. However, many mechanisms of the spatiotemporal variability of natural plankton populations are not known yet. Pronounced physical patterns like thermoclines, upwelling, fronts and eddies often set the frame for the biological process. Measurements of the underwater light field are made with state-of-the-art instruments and used to calculate concentrations of phytoplankton biomass (as chlorophyll) as well as other forms of organic matter. Very high mobility of the marine environment would prevent the formation of any stable patch spatial distribution with much longer life-time than the typical time of biodynamics. However, in addition to very changeable transient spatial patterns, there also exist other spatial patterns in marine environment, much more stable spatial structure associated with ocean fronts, spatiotemporal chaos [10, 11], cyclonic rings, and so called meddies [14]. In fact, it is significant to create the biological basis for understanding spatial patterns of plankton [15]. During a long period of time, all the spiral waves have been widely observed in diverse physical, chemical, and biological systems [16, 17, 18, 19]. However, a quite limited number of documents [11, 12, 20, 21] concern the spiral wave and their breakup in the ecological systems.

The investigation of transition from regular patterns to spatiotemporally chaotic dynamics in extended systems remains a challenge in nonlinear science [16, 22, 23]. In a nonlinear ecology system, the two most commonly seen patterns are spiral waves and turbulence. Spiral waves play an important role in ecological systems. For example, spatially induced speciation prevents the extinction of the predator-prey models [11, 12, 24]. So far, there exist various, often heuristic explanations of the breakup phenomenon, most of which consider that the spiral core is a localized source of periodic waves. Far away from the core, the profile of the spirals approaches a planar periodic wave train with a wave number specific to the parameters of the system (wavelength selection). In general, breakup is attributed to the selection of a wave number that is too small to be sustained in the system. In Refs. [22, 23], it has been argued that the spiral wavelength is already too close to the minimum wavelength λ_{min} allowed by the dispersion relation for wave trains in 1D, and two different breakup scenarios in the FitzHugh-Nagumo model. The oscillatory case shows the familiar breakup far away from the core and is related to the convective nature of the Eckhaus instability preceding the global mode instability necessary for breakup. Two main reasons for the spiral instability are found in Refs. [22, 23]: the absolute Eckhaus instability where the perturbations travel away from the spiral core and a novel finite-wavelength instability where perturbations travel towards the core. The latter instability causes spiral breakup near the core, whereas the absolute Eckhaus instability produces far-field breakup for sufficiently large group velocities of the outward propagating fastest growing modes. For oscillatory conditions, breakup of the spiral waves far away from the spiral core (as so-called "far-field breakup") was reported in a simple activator-inhibitor model by Markus Bär, Michal Or-Guil and Lutz Brusch [23], which is in the chemical reaction-

diffusion system. In present letter, the scenario in the plankton ecological system is reported. In this Letter, we find that far-field breakup of the spiral waves leading to complex spatiotemporal chaos (or a turbulentlike state) also exhibits in the plankton model in the two dimensions under the sinusoidal oscillation rather than the relaxational oscillation with large amplitude.

II. MODEL

Following Scheffer's minimal approach [25] and the Refs [10, 11, 26, 27], we study a two-variable phytoplankton and zooplankton model, describing pattern formation with the diffusion. The model is written as

$$\frac{\partial p}{\partial t} = rp(1-p) - \frac{ap}{1+bp}h + d_p\nabla^2 p, \qquad (1a)$$

$$\frac{\partial h}{\partial t} = \frac{ap}{1+bp}h - mh - f\frac{nh^2}{n^2+h^2} + d_h\nabla^2 h, \qquad (1b)$$

where the parameters are r, a, b, m, n, d_p, d_h, f, we refer to work in the Refs. [10, 11].

The local dynamics are given by

$$g_1(p,h) = rp(1-p) - \frac{ap}{1+bp}h, \qquad (2a)$$

$$g_2(p,h) = \frac{ap}{1+bp}h - mh - f\frac{nh^2}{n^2+h^2}. \qquad (2b)$$

For the non-spatial system, from the earlier results [26] by using a numerical bifurcation analysis, we know that the bifurcation and bistability can be found in the system (2) when the parameters are varied within a realistic range. For the fixed parameters (see the caption of the Fig. 1), we can see that the f controls the distance from Hopf bifurcation. For larger f, there exists only one stable steady-state, and for lowering f, at some point there is a saddle node bifurcation (SN), that is $f_{SN} = 0.658$. Then, a stable and an unstable steady-state become existence, the bistability will emerge when the parameter f is in the interval $f_{SN} > f > f_c = 0.445$ [this value is more than the Hopf onset, $f_H = 0.3397$]. There are three steady states: with these kinetics A and C are linearly stable while B is unstable. Outside this interval the system (1) has unique nontrivial fixed point. Using recent results [11], the systems (1) can well-develop the spiral waves in the oscillation regime, where the authors consider the spatial pattern when $d_p = d_h$.

Here we report the observation of spatiotemporal chaos due to breakup in the system under the $d_h \neq d_p$ case. We may now use the f and diffusion ratio, $\nu = d_h/d_p$, to evaluate the region for the spiral waves. With the help of Maple software assistance algebra computing, we obtain the spiral parameter space (f, ν) bifurcation diagrams as showing Fig. 2, in which two lines are plotted,

Hopf line and Turing lines respectively. In Fig. 2, region I denotes that the system has the homogeneous stable steady states in two dimensional spaces; II regions denote that the system has homogeneous oscillation in two dimensional spaces [28]; region III denotes that the system has spiral waves in two dimensional spaces. Noting that the region III is mixed Turing-Hopf model, in which the system generally produces the phase waves.
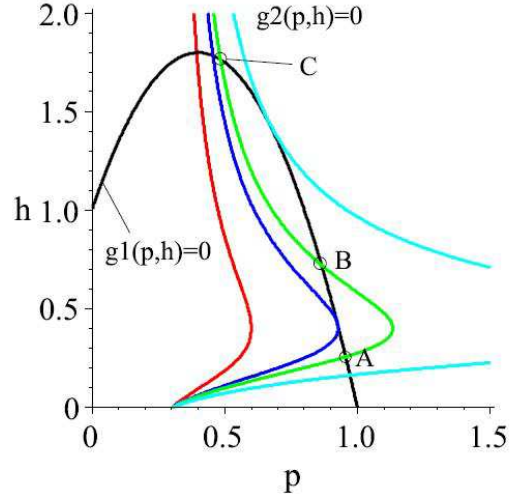

FIG. 1: The sketch map for the bistability and the Hopf bifurcation in the system (2) with $r = 5.0$, $a = 5.0$, $b = 5.0$, $m = 0.6$, and $n = 0.4$. The black curve is the $g_1(p,h)$. The colored curves are $g_2(p,h)$ with different values of f. The red curve: $f = 0.3$, the blue: $f = 0.445$, the green: $f = 0.5$ and the cyan: $f = 0.658$.
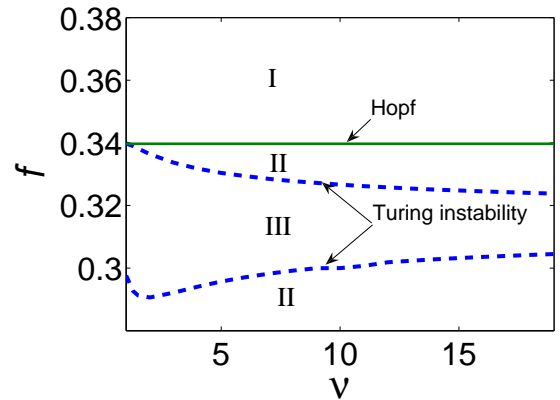

FIG. 2: The sketch map of parameter space (f, ν) bifurcation diagrams of the system (1) with $r = 5.0$, $a = 5.0$, $b = 5.0$, $m = 0.6$, $d_p = 0.05$, and $n = 0.4$.

III. NUMERICAL RESULTS

The simulation is done in a two-dimensional (2D) Cartesian coordinate system with a grid size of 600×600. The fourth order Runger-Kutta integrating method is applied with a time step $\Delta t = 0.005$ time unit and a space step $\Delta x = \Delta y = 0.20$ length unit. The results remain the same when checked by the simple Euler method. The diffusion terms in Eqs. (1a) and (1b) often describe the spatial mixing of species due to self-motion of the organism. Through the relationship between turbulent diffusion and the scale of the phenomenon in the sea [29], one can see that with the characteristic growth rate $R_0 = 10^{-5}s^{-1}$ [30] or one division per day, typical of plankton patterns d_p is about 0.05. From the biological meaning, the diffusion coefficients should satisfy $d_h \geq d_p$. However, in nature waters it is turbulent diffusion that is supposed to dominate plankton mixing [31], when $d_h < d_p$ is allowed. The other reason for choosing such parameter is that it is well-known new patterns, such as Turing patterns, can emerge in reaction-diffusion systems in which there is an imbalance between the diffusion coefficients d_p and d_h [16, 32]. Therefore, we set $\nu = d_h/d_p$, and investigated whether a spiral wave would break up into complex spatiotemporal chaos when the diffusion ratio was varied. Throughout this paper, we fix $d_p = 0.05$ and d_h is a control parameter.

In the following, we will show that the dynamic behavior of the spiral wave qualitatively change as the control parameter d_h increases from zero, i.e., the diffusion ratio ν increases from zero, to more than one. For large ν ($\nu > 1$), the outwardly rotating spiral wave is completely stable everywhere, and fills in the space when the proper parameters are chosen, as shown in Fig. 3(A). Figure 3(A) shows a series of snapshots of a well-developed single spiral wave formed spontaneously for the variable p in system (1). The spiral is initiated on a 600×600 grid by the cross-field protocol and zero boundary conditions are employed for simulations in the two dimensions. From the Fig. 3(A) we can see that the well-developed spiral waves are formed firstly by the evolution. Inside the domain, new waves emerge, but are evolved by the spiral waves growing from the center. The spiral waves can steadily grow and finally prevail over the whole domain (a movie illustrating the dynamical evolution for this case [33] [partly $movie\_1$, $movie\_2$, and $movie\_3$ for $d_h = 0.2$]). Fig. 3(B) shows that the spiral waves first break up far away from the core center and eventually relatively large spiral fragments are surrounded by a 'turbulent' bath remain. The size of the surviving part of the spiral does not shrink when d_h is further decreasing until finally d_h equals to 0, which is different from what is observed previous in the two-dimensional space Belousov-Zhabotinsky and FitzHugn-Nagumo oscillatory system [22, 23, 34, 35, 36], in which the breakup gradually invaded the stable region near the core center, and finally the spiral wave broke up in the whole medium. Figure 3(C) is the time sequences (arbitrary units) of the

variables p and h at an arbitrary spatial point within the spiral wave region, from which we can see that the spiral waves are caused by the accepted as "phase waves" with substantially group velocity, phase velocity and sinusoidal oscillation rather than the relaxational oscillation with large amplitude. This breakup scenario is similar to the breakup of rotating spiral waves observed in numerical simulation in chemical systems [22, 23, 34, 35, 36], and experiments in BZ systems [37, 38], which shows that spiral wave breakup in these systems was related to the Eckhaus instability and more important, the absolute instability.

The corresponding trajectories of the spiral core and the spiral arm (far away from the core center) at $y = 300$ are shown in Fig. 4, respectively. From Fig. 4, we can see that the spiral core is not completely fixed, but oscillates with a large amplitude. However, as d_h decreases to a critical value, an unstable modulation develops in regions which is far away from the spiral core (cf. the middle column of the Fig. 4). These oscillations eventually grow large enough to cause the spiral arm far away from the core to breakup into complex multiple spiral waves, while the core region remains stable (the corresponding movie can be viewed in the online supplemental in Ref. [33] [partly $movie\_1$ and $movie\_2$, and for $d_h = 0.02$]). Figures 3(B) and 4(B) show the dynamic behavior for $d_h = 0.02$, i.e., $\nu = 0.4$. The regular trajectories far away from the core are now the same as in the region of the spatial chaos (cf. the middle column of the Fig. 4).

Furthermore, it is well known that the basic arguments in spiral stability analysis can be carried out by reducing the system to one spatial dimension [22, 23, 34, 35, 36]. Here we show the essential properties of the spiral breakup resulting from the numerical simulation. In this model, it is worth noting that we do not neglect the oscillation of the dynamics in the core as shown in Fig. 4 when the model is simulated in one-dimension space. Breakup occurs first far away from the core (the source of waves). The spiral wave breaks towards the core until it gets to some constant distance and then the surviving part of the spiral wave stays stable. These minimal stable wavelengths are called λ_{min}. So the one-parameter family may be described by a dispersion curve $\lambda(d_h)$ (see Fig. 5). The minimal stable wavelength λ_{min} of the spiral wave in Fig. 5 comes from the simulation in two dimensional space. The results of Fig. 5 can be interpreted as follows: the minimal stable wavelengths decrease with respect to the decrease of d_h but eventually stay at a relative constant value, which is that the stable spiral waves are always existing for a larger region values of d_h. Space-time plots at different times are shown in Fig. 6 for two different d_h, i.e., different ν, which display the time evolution of the spiral wave along the cross section in the two-dimensional images of Fig. 3(A) and (B). As shown in Fig. 6(A) and (B) for $d_h = 0.2$ and $d_h = 0.02$ respectively, the waves far away from the core display unstable modulated perturbation due to convective in-
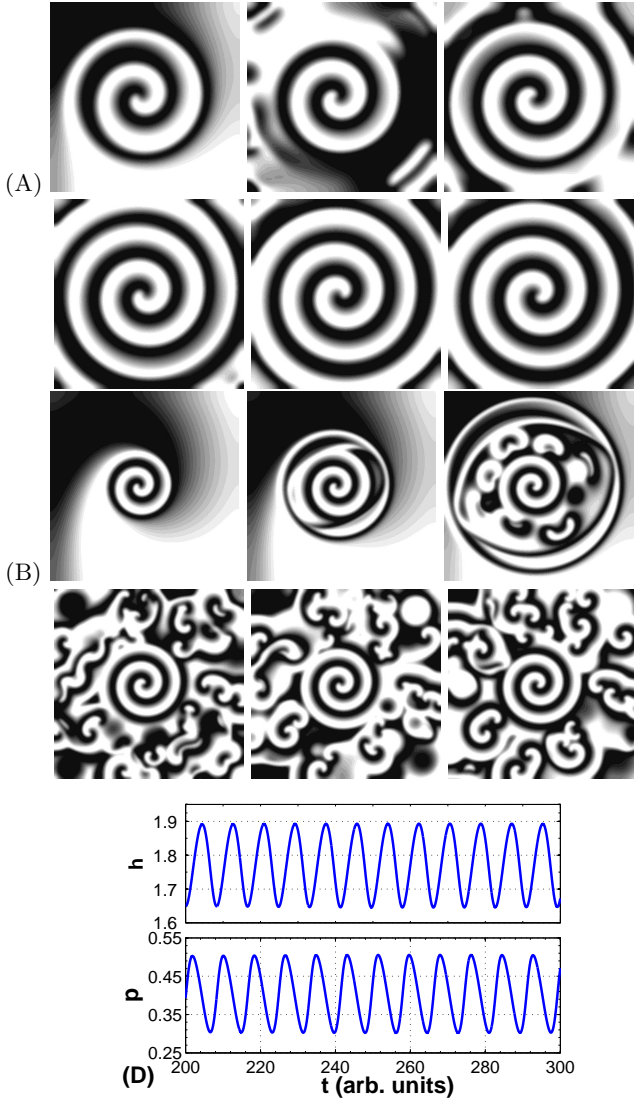
4

(D)

FIG. 3: Well developed spiral waves and some properties of them. The figures show simulations of the system (1) with $r = 5$, $a = 5$, $b = 5$, $m = 0.6$, $n = 0.4$, $d_p = 0.05$, and $f = 0.3$. (A) Well developed spiral waves shown at subsequent snapshot in time, $d_h = 0.2$. (B) Far-field breakup of the spiral waves shown at subsequent snapshot in time, $d_h = 0.02$. The white (black) areas correspond to maximum (minimum) values of p [Additional movie format available from Ref. [33]]. (C) Oscillations of the variable p and h at an arbitrary spatial point within the regular spiral wave region for both scenarios. Each figure is ran the long time until it spatial patterns are unchange.

stability [22, 23, 34, 35, 36], but this perturbation is gradually advected to the left and right sides, and finally disappears. The instability manifests itself to produce the wave train breakup several waves from the far-field, as shown in Figs. 6(B).
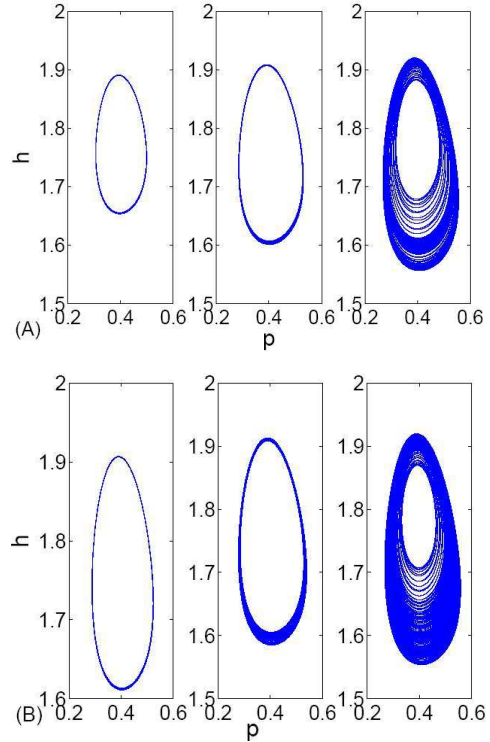

FIG. 4: The corresponding trajectories (from left to right) for locations $(300, 300)$, $(250, 300)$, and $(50, 300)$ respectively. The parameters in (A), and (B) were the same as those in Fig. 3(A) and (B), respectively.
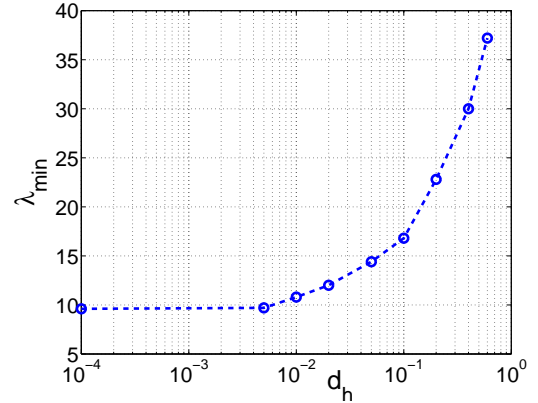

FIG. 5: Dependence of the wavelength λ_{min} on the parameter d_h for the system (1) with $r = 5.0$, $a = 5.0$, $b = 5.0$, $m = 0.6$, $d_p = 0.05$, and $n = 0.4$. Note the log scale for d_h.

IV. CONCLUSION AND DISCUSSION

We have investigated a plankton ecological system within two-dimensions pace and found that its spatial patterns exhibit spiral waves, spatial chaos patterns, and moreover, the scenario of the spatial chaos patterns obtained from the far-field breakup is observed. Our research is based on numerical analysis of a kinematic mim-
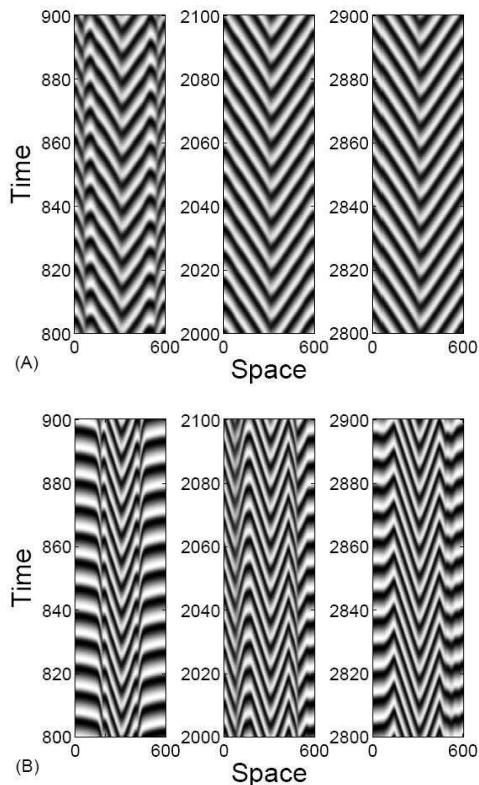
FIG. 6: Space-time plots of variable p for different time and d_h. The parameters in (A), and (B) are the same as those in Fig. 3(A) and (B), respectively.

icking the diffusion in the dynamics of marine organisms, coupled to a two component plankton model. By increasing (decreasing) the diffusion ratio of the two variables of the plankton model, the spiral arm first broke up into a turbulencelike state far away from the core center, but which do not invade the whole space. The reason causing this phenomenon can be illuminated theoretically by the M. Bär and L. Brusch study in Refs. [22, 23]. The far-field breakup can may be verified in field observation and is useful to understand the population dynamics of oceanic ecological systems. Such as that under certain conditions the interplay between wake (or ocean) structures and biological growth leads to plankton blooms inside mesoscale hydrodynamic vortices that act as incubators of primary production.

As we know that plankton plays an important role in the marine ecosystem and the climate, because of their participation in the global carbon and Nitrogen cycle at the base of the food chain [39]. From the review [40], a recently developed ecosystem model incorporates different phytoplankton functional groups and their competition for light and multiple nutrients. Simulations of those models at specific sites to explore future scenarios suggest that global environmental change, including global-warming-induced changes, will alter phytoplankton community structure and hence alter global biogeo-

chemical cycles [41]. The coupling of spatial ecosystem model to global climate raises again a series of open questions on the complexity of model and relevant spatial scales. So the study of spatial model with large-scale is more important in the ecological system. Basing on numerical simulation on the spatial model, we can draft that the oceanic ecological systems show permanent spiral waves and spatial chaos in large-scale over a range of parameter values d_h, which indicates that periodically sustained plankton blooms in the local area. The spatial chaos patterns demonstrate the perspective observation of the Fig. 3 in Ref. [40]. Also, the satellite imagery [see Fig. 7] has displayed spiral (eddy) patterns that represent the phytoplankton [the chlorophyll] biomass and thus demonstrated that plankton patterns in the ocean occur on much broader scales and therefore mechanisms thought diffusion should be considered. Where the color gives us very useful ideas of changes of the spatial patterns in chlorophyll concentrations. The more spatial patterns of the phytoplankton can be obtained from the web http://oceancolor.gsfc.nasa.gov.
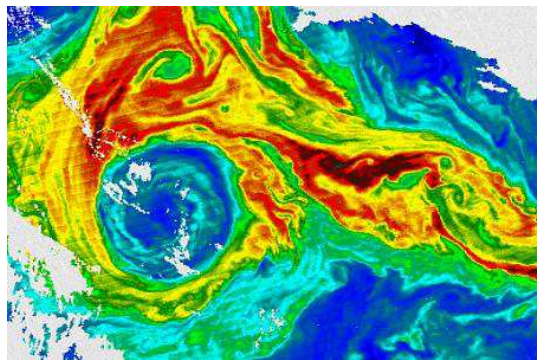

FIG. 7: This Moderate Resolution Imaging Spectroradiometer (MODIS) image shows a large eddy [about 200 kilometers in diameter] in the southwest Indian Ocean [south of Madagascar in the Agulhas Return Current region over the Southwest Indian Ridge]. The enhanced natural color image shows actual differences in water color while the pseudocolor image shows chlorophyll concentration. The images are taken form http://oceancolor.gsfc.nasa.gov, with permission from Janet W. Campbell.

[1] R. E. Amritkar and G. Rangarajan, Phys. Rev. Lett. **96**, 258102 (2006).

[2] A. Pekalski and M. Droz, Phys. Rev. E **73**, 021913 (2006).

[3] Y.-Y. H. Sayama, M. A. M. de Aguiar, and M. Baranger, FORMA **18**, 19 (2003).

[4] E. Gilad, J. von Hardenberg, A. Provenzale, M. Shachak, and E. Meron, Phys. Rev. Lett. **93**, 098105 (2004).

[5] M. J. Washenberger, M. Mobilia, and U. C. Täuber, Journal of Physics: Condensed Matter **19** (2007).

[6] M. Mobilia, I. Georgiev, and U. Täuber, Journal of Statistical Physics **128**, 447 (2007).

[7] B. Blasius, A. Huppert, and L. Stone, Nature **399**, 354 (1999).

[8] J. von Hardenberg, E. Meron, M. Shachak, and Y. Zarmi, Phys. Rev. Lett. **87**, 198101 (2001).

[9] A. Provata and G. A. Tsekouras, Phys. Rev. E **67**, 056602 (2003).

[10] A. B. Medvinsky, I. A. Tikhonova, R. R. Aliev, B.-L. Li, Z.-S. Lin, and H. Malchow, Phys. Rev. E **64**, 021915 (2001).

[11] A. B. Medvinsky, S. V. Petrovskii, I. A. Tikhonova, H. Malchow, and B.-L. Li, SIAM Review **44**, 311 (2002).

[12] W. S. C. Gurney, A. R. Veitch, I. Cruickshank, and G. McGeachin, Ecology **79**, 2516C2530 (1998).

[13] J. D. Murray, *Mathematical biology*, Interdisciplinary applied mathematics (Springer, New York, 2002), 3rd ed.

[14] L. Armi, D. Hebert, N. Oakey, J. Price, P. L. Richardson, T. Rossby, and B. Ruddick, Nature **333**, 649 (1988).

[15] E. Ranta, V. Kaitala, and P. Lundberg, Science **278**, 1621 (1997).

[16] M. C. Cross and P. C. Hohenberg, Rev. Mod. Phys. **65**, 851 (1993).

[17] K. J. Lee, R. E. Goldstein, and E. C. Cox, Phys. Rev. Lett. **87**, 068101 (2001).

[18] S. Sawai, P. A. Thomason, and E. C. Cox, Nature **433**, 323 (2005).

[19] A. T. Winfree, Chaos **1**, 303 (1991).

[20] V. N. Biktashev, J. Brindley, A. V. Holden, and M. A. Tsyganov, Chaos **14**, 988 (2004).

[21] M. Garvie, Bulletin of Mathematical Biology **69**, 931 (2007).

[22] M. Bär and L. Brusch, New Journal of Physics **6**, 5 (2004).

[23] M. Bär and M. Or-Guil, Phys. Rev. Lett. **82**, 1160 (1999).

[24] N. J. Savill and P. Hogeweg, Proceedings of the Royal Society B: Biological Sciences **265**, 25 (1998).

[25] M. Scheffer, Oikos **62**, 271 (1991).

[26] H. Malchow, Procc. R. Soc. London, Series B **251**, 103 (1993).

[27] M. Pascual, Procc. Biol. Sciences **251**, 1 (1993).

[28] Q.-X. Liu, B.-L. Li, and Z. Jin, *Resonant patterns and frequency-locked induced by additive noise and periodically forced in phytoplankton-zooplankton system* (2007).

[29] A. Okubo, *Diffusion and ecological problems: mathematical models*, Biomathematics; v. 10 (Springer-Verlag, Berlin; New York, 1980).

[30] S. E. Jørgensen and G. Bendoricchio, *Fundamentals of ecological modelling*, Developments in environmental modelling; 21 (Elsevier, Amsterdam; New York, 2001), 3rd ed.

[31] G. Sugihara and R. M. May, Nature **344**, 734 (1990).

[32] A. M. Turing, Philosophical Transactions of the Royal Society of London. Series B, Biological Sciences **237**, 37 (1952).

[33] See the movie for the evolution.

[34] F. Xie, D. Xie, and J. N. Weiss, Phys. Rev. E **74**, 026107 (2006).

[35] B. Sandstede and A. Scheel, Phys. Rev. E **62**, 7708 (2000).

[36] S. M. Tobias and E. Knobloch, Phys. Rev. Lett. **80**, 4811 (1998).

[37] Q. Ouyang and J. M. Flesselles, Nature **379**, 143 (1996).

[38] Q. Ouyang, H. L. Swinney, and G. Li, Phys. Rev. Lett. **84**, 1047 (2000).

[39] J. Duinker and G. Wefer, Naturwissenschaften **81**, 237 (1994), 10.1007/BF01131574.

[40] M. Pascual, Plos Computational Biology **1**, 101 (2005).

[41] E. Litchman, C. A. Klausmeier, J. R. Miller, O. M. Schofield, and P. G. Falkowski, Biogeosciences **3**, 585 (2006).